

defects in quasicrystals, revisited

II— perfect and imperfect dislocations

Maurice Kleman*

Institut de Physique du Globe de Paris — Sorbonne Paris Cité
1, rue Jussieu - Paris cedex 05, France

March 22, 2013

Contents

1	introduction	2
2	perfect and imperfect dislocations in a QC	3
2.1	true sites and false sites in $E_{ }$	3
2.2	true sites and false sites mapped onto E_{\perp}	4
2.3	false sites and matching faults: flipping vectors	6
2.4	VP for general matching faults	9
3	glide and climb	10
3.1	glide	10
3.2	climb	11
4	discussion	12

*kleman@ipgp.fr

Abstract

In this paper, the second part of a survey of the geometric properties of defects in quasicrystals studied from the Volterra viewpoint (see ref. [1]), we show that: 1— a disvection line $L_{||} \subset E_{||}$ of Burgers vector $\mathbf{b} = \mathbf{b}_{||} + \mathbf{b}_{\perp}$ splits naturally along $L_{||}$ into a perfect dislocation of Burgers vector $\mathbf{b}_{||}$ and an imperfect dislocation of Burgers vector related to \mathbf{b}_{\perp} , akin to a stacking fault, (a 'phason' defect), 2— the 'phason' defects are classified according to the relative position of Σ_{\perp} with respect to a partition of the acceptance window AW which depends on the direction of \mathbf{b}_{\perp} . The perpendicular cut surface $\Sigma_{\perp} \subset AW$ here introduced is a mapping of the usual cut surface $\Sigma_{||} \subset E_{||}$. Imperfect dislocations in QCs are somewhat similar to Kronberg's synchroshear dislocations. It is also shown that climb must generically be easier than glide.

1 introduction

It has been shown in a previous paper [1] (hereunder denoted (I)) that quasicrystal rational approximants result from a periodic distribution of flips on the parent QC structure. When only one flip per unit cell, one gets the so-called Fibonacci approximants. A flip is not a topological defect and can be split into two opposite matching faults, which are topological defects; this is most probably the situation in stable approximants. A matching fault has all the characteristics of a usual stacking fault in a crystal; as we shall see it carries an effective Burgers vector $\mathbf{b}_{||}^{eff} \subset E_{||}$ which expression will be derived from a geometrical analysis in E_{\perp} .¹

The approach to dislocations we favor in the present article is based on a Volterra process [2] carried out in $E_{||}$, not in \mathcal{E} . In the latter process, which at first sight might seem more natural, the resulting defects show up as the intersection of the defect in $\mathcal{E} = E_{||} \times E_{\perp}$ and $E_{||}$. But this method, employed e.g. in [3] and made easy to-day by the powerful computer simulations at our disposal, does not show up at once why disvections (as we call the set of defects carried by a dislocation $L_{||} \subset E_{||}$, Burgers vector $\mathbf{b} = \mathbf{b}_{||} + \mathbf{b}_{\perp}$) is split in $E_{||}$ into two types of line defects, akin respectively to perfect dislocations (all of Burgers vectors $\mathbf{b}_{||}$) and imperfect dislocations (whose Burgers vectors measured in $E_{||}$ depend on \mathbf{b}_{\perp} , but vary in a subtle way according to the position of the line defect). Thus a unique disvection generically shows

¹The notations are the same as in (I).

up in physical space as a cloud of matching faults accompanying a perfect dislocation line.

Sect. 2.1 and 2.2 introduce the main concept at work in this paper, namely the distinction between **true sites** and **false sites** of the cut surface $\Sigma_{||}$ in $E_{||}$ for a defect line $L_{||}$; their consideration leads straight to the distinction between perfect and imperfect dislocations (stacking faults). Perfect and imperfect dislocations do not mix along $L_{||}$; they separate in space. This is indeed what is observed empirically.

Sect. 2.3 and 2.4 develop a geometric method to obtain the Burgers vector of a matching fault; it depends on \mathbf{b}_{\perp} and on the location of $L_{||}$. The essential ingredient is the concept of **flipping vector**.

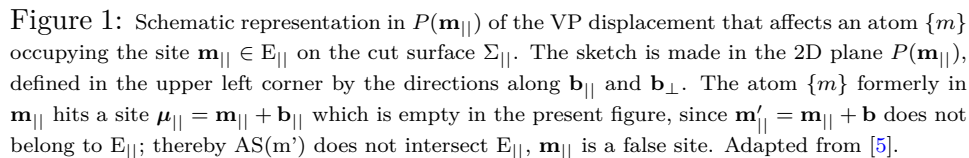
In Sect. 3 we show that, within the present analysis, climb appears as easier than glide, a result experimentally well attested [4].

2 perfect and imperfect dislocations in a QC

2.1 true sites and false sites in $E_{||}$

A VP performed in a 3D *periodic* crystal moves any atom $\{m\}$ occupying any site $\mathbf{m} \in \Sigma$, the cut surface, to a site $\boldsymbol{\mu} = \mathbf{m} + \mathbf{b}$ either occupied by an atom $\{\mu\}$ crystallographically equivalent to $\{m\}$, – this is a **perfect dislocation** –, or occupied by an unequivalent atom (or not occupied at all), – this is an **imperfect dislocation**. We call \mathbf{m} a **true site** in the first case, a **false site** otherwise; all the sites are either false or true, depending on \mathbf{b} .

The same distinction can be made in a quasicrystal for the physical Burgers vector $\mathbf{b}_{||}$, but in this case the same cut surface $\Sigma_{||}$ can accommodate both types of sites. Figure 1 represents the case of a false site; let $P(\mathbf{m}_{||}) \subset \mathcal{E}$ a 2D plane that contains the QC site $\mathbf{m}_{||}$ and the two directions along $\mathbf{b}_{||}$ and \mathbf{b}_{\perp} ; they play different roles and are thus conveniently separated. $AS(\mathbf{m})$ is the atomic surface for the atom $\{m\}$ located at the site $\mathbf{m}_{||}$, \mathbf{m} is the center of the hyperlattice cell to which $AS(\mathbf{m})$ is attached. $AS(\mathbf{m})$ intersects $P(\mathbf{m}_{||})$ along a segment denoted $AS^1(\mathbf{m})$, smaller in length than or equal to the span of $AS(\mathbf{m})$ projected onto $P(\mathbf{m}_{||})$, $AS^1(\mathbf{m}) \in AS(\mathbf{m})$. $\mathbf{m}' = \mathbf{m} + \mathbf{b}$; in Fig. 1 $AS(\mathbf{m}')$ does not intersect $E_{||}$, $\mathbf{m}_{||}$ is thus a false site.



Now we characterize the true and false sites by their projections onto the perpendicular space E_{\perp} . For the sake of illustration we assume in the sequel that the hyperspace is 4-dimensional, $d = 4$, $d_{\parallel} = d_{\perp} = 2$, and that the symmetry is octagonal; the results extend easily to any dimension $d = d_{\parallel} + d_{\perp}$.

4

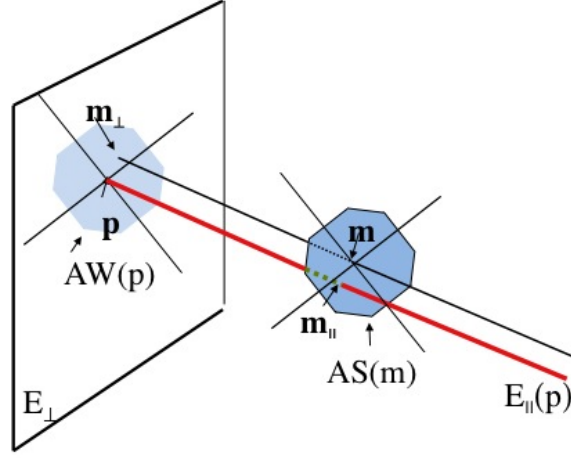


Figure 2: Octagonal symmetry, $d = 4$. The 2-dimensional physical plane $E_{\parallel}(\mathbf{p})$, that intersects orthogonally E_{\perp} in one point only, \mathbf{p} , is represented as a line. The acceptance window $AW(\mathbf{p})$ is the closure of the hypercube center projections \mathbf{m}_{\perp} whose attached $AS(\mathbf{m})$ s intersect E_{\parallel} . These projections fill AW densely. Adapted from [5].

false whether they derive from a true or false site \mathbf{m}_{\parallel} .² Denote $\partial\Sigma_{\perp} = L_{\perp}$ the boundary of Σ_{\perp} ; even though Σ_{\perp} can be chosen at will, its border L_{\perp} , which is one-to-one with L_{\parallel} , is fixed.

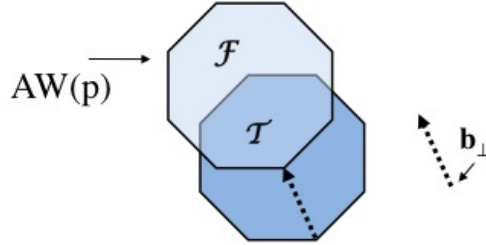


Figure 3: For the \mathbf{b}_{\perp} vector indicated, the acceptance window divides into two regions: \mathcal{T} , where the sites are true, and \mathcal{F} , where the sites are false. See text.

The true sites belong to a subset of AW , denoted \mathcal{T} , and the false sites to its complement \mathcal{F} in AW , see Fig. 3.³ \mathcal{T} is the intersection of AW and of a copy of AW translated by $-\mathbf{b}_{\perp}$. It is easy to check that, if it is so, any point $\mathbf{m}_{\perp} \in \mathcal{T}$ is displaced by the VP to a point $\mathbf{m}'_{\perp} = \mathbf{m}_{\perp} + \mathbf{b}_{\perp}$ which is still

²The same point in AW is a possible projection of several *continuous* sites \mathbf{m} belonging to Σ and defined by interpolation. We do not take into account such a complication, which does not invalidate the reasonings that follow.

³This figure rectifies an error in fig. 7, ref. [5], from which it is adapted.

in AW; it is a true site since the attached atomic surface $AS(m')$ intersects $E_{||}$. Likewise any point $\mathbf{m}_{\perp} \in \mathcal{F}$ is displaced to a point outside AW and is a false site.

If $\Sigma_{\perp} \subset AW$ is entirely in \mathcal{T} (resp. \mathcal{F}), then L_{\perp} is entirely in \mathcal{T} (resp. \mathcal{F}), i.e. L_{\perp} is true, there are no matching faults attending the perfect dislocation $\mathbf{b}_{||}$ (resp. L_{\perp} is false and the dislocation is imperfect). Generically a disvection can be separated into a perfect and an imperfect dislocation, by introducing two segments of opposite signs along the boundary $\{\mathcal{T}, \mathcal{F}\}$ between \mathcal{T} and \mathcal{F} . This is sketched Fig. 4 for the octagonal case, with pointlike dislocations.

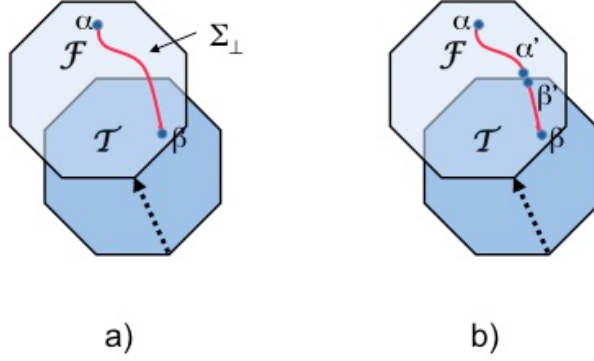


Figure 4: a) dipole with two opposite pointlike dislocations α, β , cut surface Σ_{\perp} , here a line segment; b) the same dipole split into a perfect dipole β, β' and a matching fault α, α' .

2.3 false sites and matching faults: flipping vectors

Fig. 3 shows that if \mathbf{b}_{\perp} is equal to the span of $AW(p)$ or larger, then $\mathcal{T} = \emptyset$, $AW = \mathcal{F}$; the disvection is reduced to a matching fault, whatever the shape of $L_{||}$ may be.

Let us define more precisely the relation between such a \mathbf{b}_{\perp} — we take it equal to the span \mathbf{b}_{\perp}^* in Fig. 5a — and an imperfect dislocation. In the octagonal case there are four such vectors; the corresponding hypervectors $\mathbf{b}^* = \mathbf{b}_{||}^* + \mathbf{b}_{\perp}^*$ join parallel edges of the 4D hypercells. In the general case of a d -hyperspace they join opposite $(d_{\perp} - 1)$ -dimensional faces.

They can be called **flipping vectors**, since they put in correspondence two points on the boundary of $AW(p)$, one of which deriving from a false $\mathbf{m}_{||}$

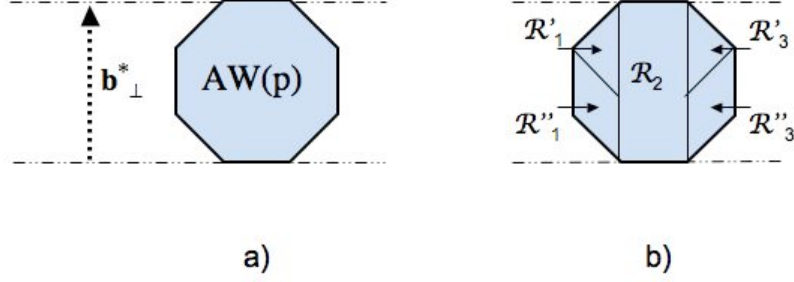


Figure 5: Octagonal case. a) one of the four basic flipping vectors in P_\perp , b) partition of AW related to \mathbf{b}_\perp^* , see text.

for the Burgers vector \mathbf{b}^* , the other one from an empty site $\boldsymbol{\mu}_\parallel = \mathbf{m}_\parallel + \mathbf{b}_\parallel^*$. Notice that in the Fig. 2 of (I) the vector joining the centers of the atomic surfaces C_3^- and C_3^+ is such a vector. Flipping vectors are also related to the *silhouetting* d_\parallel -planes of Frenkel & al. [6], which project onto E_\perp along the boundary of the acceptance window AW(p). A flipping vector \mathbf{b}^* is precisely a vector that joins the centers of two hypercubes that have a $(d_\perp - 1)$ -dimensional face in common; they are tabulated in [6] for the Penrose and the icosahedral QCs.

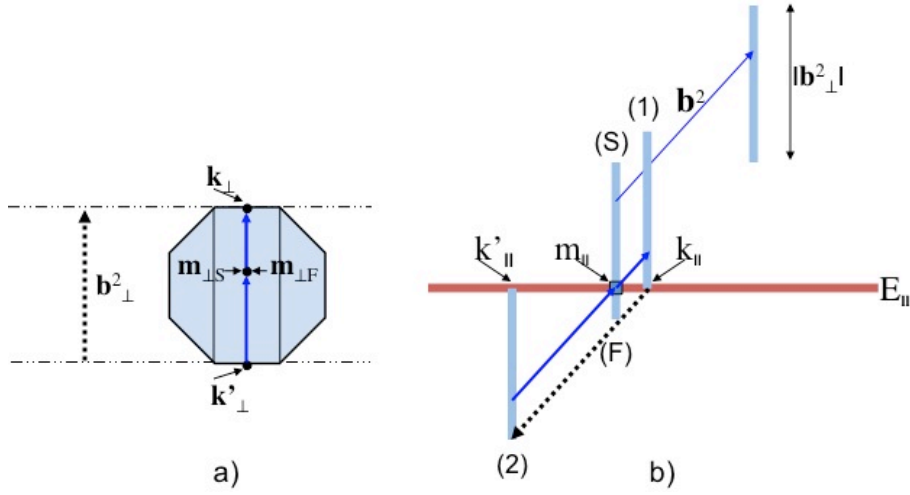


Figure 6: Octagonal case. a) displacement of $\{m\}$ in E_\perp from $\mathbf{m}_{\perp S}$ to $\mathbf{m}_{\perp F}$; here $\mathbf{m}_{\perp S}$ and $\mathbf{m}_{\perp F}$ occupy the same site \mathbf{m}_\perp ; b) displacement of $\{m\}$ in $P(\mathbf{m}_\parallel)$, see text.

Then, what is a stacking fault whose Burgers vector is a flipping vector? We are guided in this search by the two representations we have already

used for the displacement of an atomic surface $AS(m)$ with $\{m\} \in \Sigma$, one in the perpendicular space E_{\perp} – the displacement of \mathbf{m}_{\perp} –, the other in $P(\mathbf{m}_{\parallel})$ – the displacement of \mathbf{m}_{\parallel} , both rather simple in the case in view. The \mathbf{m}_{\perp} representation will appear more manageable in more complicated cases.

There are several situations according to the position of \mathbf{m}_{\perp} in AW, see the relevant partition in Fig. 5b and explanations hereunder.

– Consider first an atom $\{m\}$ represented in AW by the site $\mathbf{m}_{\perp S} \in \mathcal{R}_2$ from which the displacement starts, Fig. 6a. This displacement brings $\{m\}$ to a site \mathbf{k}_{\perp} on the boundary of AW, where it has to flip to the site $\mathbf{k}'_{\perp} = \mathbf{k}_{\perp} - \mathbf{b}_{\perp}^2$; it then continues its displacement up to a final site $\mathbf{m}_{\perp F}$ to complete it to the value of the Burgers vector, the flipping displacement $\mathbf{k}_{\perp} \mathbf{k}'_{\perp}$ not being taken into account: in the present case the final site $\mathbf{m}_{\perp F} = \mathbf{m}_{\perp S}$, the total shift in E_{\perp} is thus equal to the flipping displacement.

The same result holds when one considers the displacement in $P(\mathbf{m}_{\parallel})$, see Fig. 6b: $AS(m)$ is represented by its intersection with $P(\mathbf{m}_{\parallel})$, whose span is exactly $|\mathbf{b}_{\perp}^2|$; it is displaced by the VP from position (S) where $AS(m)$ intersects E_{\parallel} in m_{\parallel} to position (1) from which it flips to (2) and then completes its displacement by going to (F), which is also (S) in the present case. The total displacement, not taking the flip into account, vanishes. Thus the Burgers vector of the dislocation in physical space is \mathbf{b}_{\parallel}^2 , and is attended by a stacking fault whose shift is \mathbf{b}_{\parallel}^2 . This is much comparable to a partial dislocation in a periodic crystal; this is also the simplest case of imperfect dislocation one can meet in a QC.

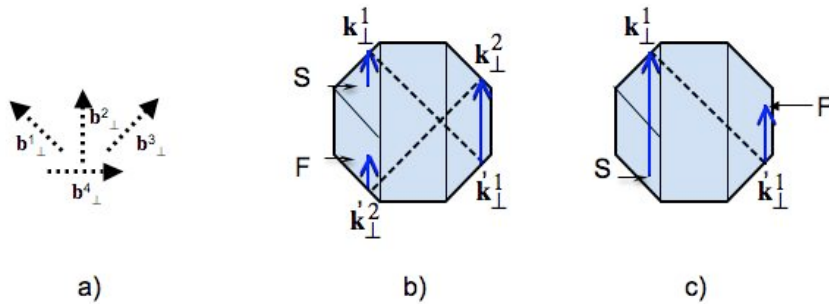


Figure 7: a) directions of the flipping vectors; b) $\mathbf{m}_{\perp} \in \mathcal{R}'_1$. There are two flips: $-\mathbf{b}_{\perp}^1$ and $-\mathbf{b}_{\perp}^3$, $\mathbf{b}^{eff} = \mathbf{b}^2 - \mathbf{b}^1 - \mathbf{b}^3$, $\mathbf{SF} = (1 - \sqrt{2}) \mathbf{b}_{\perp}^2$; c) $\mathbf{m}_{\perp} \in \mathcal{R}''_1$. One flip only: $-\mathbf{b}_{\perp}^1$, $\mathbf{b}^{eff} = \mathbf{b}^2 - \mathbf{b}^1$.

– \mathcal{R}_1 and \mathcal{R}_3 being equivalent under a transposition, we turn our atten-

tion to \mathcal{R}_1 only; the stages of the displacement of the cut surface atoms are sketched in Fig. 7. There are in fact two cases:

– \mathbf{m}_\perp is in S (starting point) in \mathcal{R}'_1 , the triangular region in the upper part of \mathcal{R}_1 . In that case the atom meets the boundary of AW after a rather short run, and two flips are necessary for a displacement $\mathbf{b}_\perp^2 = \mathbf{S}\mathbf{k}_\perp^1 + \mathbf{k}_\perp'^1\mathbf{k}_\perp^2 + \mathbf{k}_\perp'^2\mathbf{F}$. The effective Burgers' vector, flips included, is

$$\mathbf{b}_\parallel^{eff} = \mathbf{b}_\parallel^2 - \mathbf{b}_\parallel^1 - \mathbf{b}_\parallel^3 \quad (1)$$

in the physical space E_\parallel . The flips define the matching fault shift,

– \mathbf{m}_\perp is in S (starting point) in \mathcal{R}''_1 , the parallelogram in the lower part of \mathcal{R}_1 . Then $\mathbf{S}\mathbf{k}_\perp^1$ is larger than in the former case, and the displacement $\mathbf{b}_{2\perp} = \mathbf{S}\mathbf{k}_\perp^1 + \mathbf{k}_\perp'^1\mathbf{F}$. There is only one flip, and the effective Burgers' vector, flip included, is

$$\mathbf{b}_\parallel^{eff} = \mathbf{b}_\parallel^2 - \mathbf{b}_\parallel^1. \quad (2)$$

Here again, the flips define the matching fault shift,

2.4 VP for general matching faults

The general case for $|\mathbf{b}_\perp| < |\mathbf{b}_\perp^*|$ can be easily treated, on the same basis as the case of flipping vectors, see Fig. 8. Starting from the site $\mathbf{m}_{\perp S} \in \mathcal{F}$, \mathbf{b}_\perp hits the boundary in \mathbf{k}_\perp^1 , flips to $\mathbf{k}_\perp'^1$, from which site it reaches $\mathbf{m}_{\perp F}$. Notice that $|\mathbf{k}_\perp'^1\mathbf{k}_\perp^2| < |\mathbf{b}_\perp|$, since by construction the width of \mathcal{F} in the direction of \mathbf{b}_\perp is precisely $|\mathbf{b}_\perp|$. Therefore $\mathbf{m}_{\perp F} \in \mathcal{F}$, and there is no necessity for a second flip. Thus, in the case of the octagonal AW of Fig. 8:

$$\mathbf{b}_\perp^{eff} = \mathbf{b}_\perp - \mathbf{b}_\perp^1 \rightarrow \mathbf{b}_\parallel^{eff} = \mathbf{b}_\parallel - \mathbf{b}_\parallel^1. \quad (3)$$

The position of $\mathbf{m}_{\perp S}$ in \mathcal{F} determines which edge of the octagon \mathbf{b}_\perp hits; thus there are four types of matching faults associated to \mathbf{b}_\perp , namely,

$$\mathbf{b}_\parallel - \mathbf{b}_\parallel^1, \mathbf{b}_\parallel - \mathbf{b}_\parallel^2, \mathbf{b}_\parallel - \mathbf{b}_\parallel^3, \mathbf{b}_\parallel + \mathbf{b}_\parallel^4, \quad (4)$$

(cf. Fig. 7 for the orientations of the flipping vectors). Again, the flips define the matching fault shifts.

The position of $\mathbf{m}_{\perp S}$ in \mathcal{F} determines which edge of the octagon \mathbf{b}_\perp hits; thus there are four types of matching faults associated to \mathbf{b}_\perp , namely,

$$\mathbf{b}_\parallel - \mathbf{b}_\parallel^1, \mathbf{b}_\parallel - \mathbf{b}_\parallel^2, \mathbf{b}_\parallel - \mathbf{b}_\parallel^3, \mathbf{b}_\parallel + \mathbf{b}_\parallel^4, \quad (5)$$

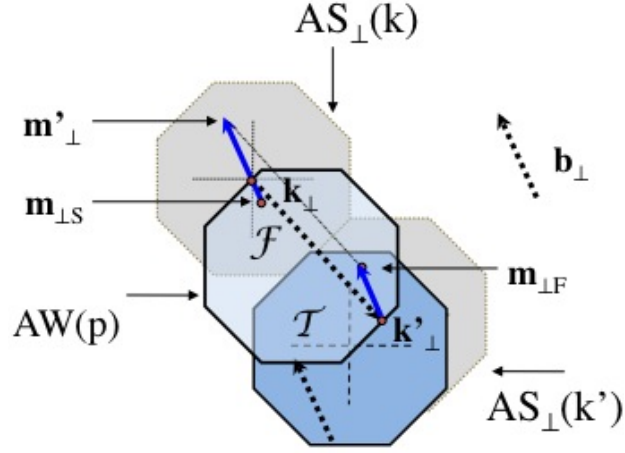


Figure 8: VP for a false site, see text.

(cf. Fig. 7 for the orientations of the flipping vectors), Fig. 9a. This is true (and extends to any quasicrystal) except if \mathbf{b}_\perp is parallel to one of the edges, in which case there are only three exits possible for \mathbf{b}_\perp , Fig. 9b.

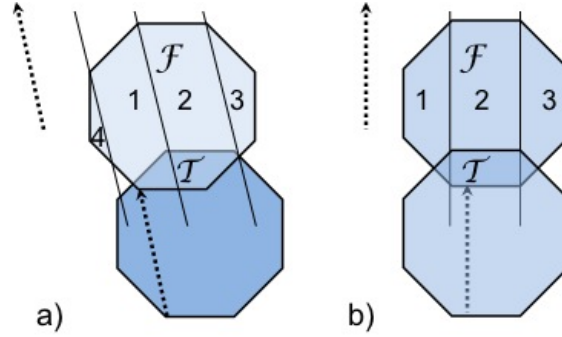


Figure 9: The various types of matching faults: a) for a Burgers vector \mathbf{b}_\perp oblique with respect to all the edges, b) for a Burgers vector parallel to one of the edges.

3 glide and climb

3.1 glide

In accordance with the standard definition of the glide plane of a dislocation line in a classic 3D crystal – the glide plane contains the dislocation line and the direction of the Burgers vector – we define the glide manifold

$G = L \times \langle \mathbf{b} \rangle$ of a dislocation in a d -dimensional crystal as the cartesian product of the $(d - 2)$ -dimensional dislocation hyperline $L = L_{||} \times E_{\perp}$ (cf. [3]) by the straight line along the direction of the Burgers vector \mathbf{b} .⁴ This definition holds for a straight dislocation or along a small segment of a curved dislocation.

Any movement of L in G along \mathbf{b} is accompanied by a movement of $L_{||}$ in $G_{||} = L_{||} \times \langle \mathbf{b}_{||} \rangle$, the glide plane in $E_{||}$, along $\mathbf{b}_{||}$ (more precisely along the direction of the edge component \mathbf{b}_e of $\mathbf{b}_{||}$). Indeed, the glide manifold G in E can be written:

$$(L_{||} \times E_{\perp}) \times \langle \mathbf{b} \rangle = (L_{||} \times \langle \mathbf{b} \rangle) \times E_{\perp} = (L_{||} \times \langle \mathbf{b}_{||} \rangle) \times E_{\perp} = G_{||} \times E_{\perp},$$

the penultimate equality resulting from $\mathbf{b}_{\perp} \in E_{\perp}$. By definition, $G_{||} = L_{||} \times \langle \mathbf{b}_{||} \rangle$ is the usual physical glide plane; thereby our definition of the glide manifold G is consistent with the definition of the glide plane $G_{||}$ of the physical dislocation line. Also, $G_{||} = L_{||} \times \mathbf{b}_e$.

Consider now the modification of the cut surface $\Sigma_{||} \subset E_{||}$ under glide and the effect on $\Sigma_{\perp} \subset E_{\perp}$, e.g. in Fig. 4. As $L_{||}$ is displaced along \mathbf{b}_e , it meets a certain number of atoms $\{m\}$ – added to the cut surface $\Sigma_{||}$ – that carry atomic surfaces of centers \mathbf{m} ; are also added, by interpolation as above, virtual atomic surfaces attached to the continuous positions visited by the moving $L_{||}$. This allows us to define a continuous set of projections \mathbf{m}_{\perp} on $AW(p)$. If the displacement of $L_{||}$ takes a 'full' value \mathbf{b}_e (or $\mathbf{b}_{||}$, which is equivalent), the displacement in $AW(p)$ is equal to \mathbf{b}_{\perp} , i.e. necessarily a false site for $\beta'' = \beta' + \mathbf{b}_{\perp}$, which result is visible from the inspection of Fig. 4b; by interpolation there is a continuous path between β' and β'' which is entirely in \mathcal{F} . Thus 'phason' defects (imperfect dislocations) are generically produced by glide.

3.2 climb

Climb is of another nature. Pure climb in the hypercrystal is a displacement of the hyperline L along a well defined direction $\langle \mathbf{c} \rangle$ that is perpendicular both to L and to \mathbf{b} . Since E_{\perp} belongs to L , $\langle \mathbf{c} \rangle$ is perpendicular to E_{\perp} , and thus belongs to the physical space $E_{||}$. In order to fully achieve the orthogonality of $\langle \mathbf{c} \rangle$ to \mathbf{b} and to L , it is then enough that $\langle \mathbf{c} \rangle$

⁴ $\langle \mathbf{a} \rangle$ denotes a unsigned infinite line in the direction of \mathbf{a} .

be perpendicular to $\mathbf{b}_{||}$ and to $L_{||}$. Therefore pure climb in physical space is along $\langle \mathbf{c} \rangle$, and is thus the same process as pure climb in the hypercubic lattice.

Let $\gamma_{||}$ be the amount of climb along $\langle \mathbf{c} \rangle$; any atom met along $\langle \mathbf{c} \rangle$ (real or interpolated) is defined by its position $\gamma_{||}$ and its atomic surface with center $\gamma = \gamma_{||} + \gamma_{\perp}$. By the definition of climb in the hyperlattice, one has $\gamma \cdot \mathbf{b} = 0$; likewise, by the definition of climb in the physical space, $\gamma_{||} \cdot \mathbf{b}_{||} = 0$. Thus one gets

$$\gamma_{\perp} \cdot \mathbf{b}_{\perp} = 0;$$

thus the displacement of β' to β'' ($\beta'' = \beta' + \gamma_{\perp}$) locates β'' close to the boundary between \mathcal{T} and \mathcal{F} , either in \mathcal{F} or in \mathcal{T} . According to the sign of γ_{\perp} , climb is accompanied by the formation of imperfect dipoles (a small amount) or no dipoles at all. This seems to indicate that climb is more favored in one direction.

4 discussion

The $\mathbf{b}_{||}$ dislocations are singularities *per se*, since the cloud of accompanying matching faults can be erased by opposite matching faults or by diffusion [7]. Thus there is a topological classification of the dislocations $\mathbf{b}_{||}$ alone [8]. Similarly, as pointed out in (I), there is a topological classification of the matching faults. These two classifications can be given a unique framework for \mathbf{b} [8]: but whereas crystal dislocation lines relate to a group of commutative translation symmetries, quasicrystal disvections relate to a group of non-commutative **transvection symmetries** (Cartan's [9]), thus their name. The VP provides a simpler, more physical picture.

Because the 'phason' defects are imperfect dislocation dipoles that relax the long range 'phonon' stresses of perfect dislocations, glide in a QC shows some analogy with Kronberg's synchroshear [10], where dislocation glide is assisted by shifts of the smaller atoms, yielding partial companion dipoles. However, since climb is an easier process than glide, the question remains open whether the formation of imperfect dipoles is easier by synchroclimb rather than by synchroshear, or whether a high activation energy for synchroclimb definitely makes certain that climb is favored in one direction only.

The octagonal case is rather easy to treat conceptually, and this might encourage experiments (observation of defects) in this type of structure.

acknowledgments

I thank Jacques Friedel for encouragements – for this part and for part (I).

This is IPGP contribution # 3384.

References

- [1] M. Kleman. Defects in quasicrystals, revisited: I– flips, approximants, phason defects. 2013. submitted.
- [2] J. Friedel. *Dislocations*. Pergamon Press, London, 1964.
- [3] M. Kleman and C. Sommers. Dislocations in a Penrose tiling. *Acta Met. Mat.*, 39:287–293, 1991.
- [4] D. Caillard, G. Vanderschaeve, L. Bresson, and D. Gratias. Transmission electronic microscopy study of dislocations and extended defects in as-grown icosahedral Al-Pd-Mn single grains. *Phil. Mag. A*, 80:237–253, 2000.
- [5] M. Kleman. Phasons and the plastic deformation of quasicrystals. *Eur. Phys. J. B*, 31:315–325, 2003.
- [6] D. M. Frenkel, C. L. Henley, and E. D. Siggia. Topological constraints on quasicrystal transformations. *Phys. Rev. B*, 34:3649–3669, 1986.
- [7] M. Feuerbacher and D. Caillard. Dynamics of phason diffusion in icosahedral Al-Pd-Mn quasicrystals. *Acta Mat.*, 54:3233–3240, 2006.
- [8] M. Kleman. Dislocations and disvections in aperiodic crystals. *J. Phys. I France*, 2:69–87, 1992.
- [9] E. Cartan. *Leçons sur la géométrie des espaces de Riemann*. Gauthier-Villars, Paris, 1963.
- [10] M. L. Kronberg. Plastic deformation of single crystals of sapphire. Basal slip and twinning. *Acta Metall.*, 5:507–524, 1957.